On the Dynamic Properties of Flexible Parallel Manipulators in the Presence of Type 2 Singularities

Sébastien Briot[1]
Institut de Recherches en Communications
et Cybernétique,
de Nantes (IRCCyN),
UMR CNRS 6597,
1 rue de la Noë, BP 92101,
44321 Nantes Cedex 3, France
e-mail: Sebastien.Briot@irccyn.ec-nantes.fr

Vigen Arakelian
Département de Génie Mécanique
et Automatique - L.G.C.G.M. EA3913,
Institut National des Sciences Appliquées
(I.N.S.A.),
20 avenue des Buttes de Coësmes – CS 14315,
F-35043 Rennes, France
e-mail: vigen.arakelyan@insa-rennes.fr

In the present paper, we expand information about the conditions for passing through Type 2 singular configurations of a parallel manipulator. It is shown that any parallel manipulator can cross the singular configurations via an optimal control permitting the favorable force distribution, i.e., the wrench applied on the end-effector by the legs and external efforts must be reciprocal to the twist along with the direction of the uncontrollable motion. The previous studies have proposed the optimal control conditions for the manipulators with rigid links and flexible actuated joints. The different polynomial laws have been obtained and validated for each examined case. The present study considers the conditions for passing through Type 2 singular configurations for the parallel manipulators with flexible links. By computing the inverse dynamic model of a general flexible parallel robot, the necessary conditions for passing through Type 2 singular configurations are deduced. The suggested approach is illustrated by a 5R parallel manipulator with flexible elements and joints. It is shown that a 16th order polynomial law is necessary for the optimal force generation. The obtained results are validated by numerical simulations carried out using the software ADAMS. [DOI: 10.1115/1.4004229]

Keywords: singularity, dynamics, parallel manipulators, optimal motion generation, flexible links

1 Introduction

There are many studies dealing with the singularity analysis of parallel manipulators and an overview of all the works seems almost impossible within the framework of this paper. Let us disclose the kinematic, kinetostatic, and dynamic aspects of singularity through some of them. The analysis of singular configurations has been first discussed from a kinematic point of view [1]–[12]. However, it is also known that, when parallel manipulators have Type 2 singularities [1], they lose their stiffness and their quality of motion transmission, and as a result, their payload capability. Therefore, the singularity zones in the workspace of manipulators may be analyzed not only in terms of kinematic criterions, from the theoretically perfect model of manipulators without friction and force transmission action, but also in terms of kinetostatic performance [13]–[20]. In this vein, the paper [20] proposes the analysis and design of a Stewart platform based force–torque sensor in a near-singular configuration. It was shown in this study that various singular configurations can be obtained to get high sensitivity to various combinations of the six components of force and torque.

The further study of singularity in parallel manipulators has revealed an interesting problem that concerns the path planning of parallel manipulators under the presence of singular positions, i.e., the motion feasibility in the neighborhood of singularities. In this case the dynamic conditions can be considered in the path planning process. One of the most evident solutions for the stable motion generation in the neighborhood of singularities is to use redundant sensors and actuators [21]–[25]. However, it is an expensive solution to the problem because of the additional actuators and the complicated control of the manipulator caused by actuation redundancy. Another approach concerns with motion planning to pass through singularity [26]–[31], i.e., a parallel manipulator may track a path through singular poses if its velocity and acceleration are properly constrained. This is a promising way for the solution of this problem. However, the studies devoted to this problem have addressed the path planning for obtaining a good tracking performance, but not the physical interpretation of dynamic aspects.

The condition of optimal force generation in rigid parallel manipulators for passing through the singular positions has been studied in Ref. [32]. It was shown that any parallel manipulator can pass through the singular positions without perturbation of motion if the wrench applied on the end-effector by the legs and external efforts of the manipulator are reciprocal to the twist along the direction of the uncontrollable motion. The obtained results were validated through experimental tests carried out on the prototype of 4 degree of freedom (DOF) parallel manipulator PAMINSA [33].

This approach has been generalized in the case of rigid-link flexible-joints parallel manipulators [34]. It was shown that the degree of the polynomial law should be different, when the flexibility of actuated joints is introduced into condition of the optimal force generation in the presence of singularity. The numerical simulations carried out using the software ADAMS validated the obtained theoretical results.

The study presented in this paper is the continuation of our previous works [32,34]. The purpose of this paper is to study the dynamic properties of parallel manipulators not only having flexible joints but also flexible links.

The paper is organized as follows. Section 2 presents theoretical aspects of the examined problem, which is analysed using the Lagrangian formulation. The condition of force distribution is

[1]Corresponding author.

Contributed by the Mechanisms and Robotics Committee of ASME for publication in the Journal of Mechanisms and Robotics. Manuscript received October 5, 2010; final manuscript received April 21, 2011; published online August 10, 2011. Assoc. Editor: Jean-Pierre Merlet.

defined, that allows the passing of any flexible parallel manipulator through the Type 2 singular positions. In Sec. 3, the suggested solution is illustrated via a 5*R* planar parallel manipulator having flexible links and joints. Conclusions are presented at the end of the paper.

2 Optimal Dynamic Conditions for Passing Through Type 2 Singularity

Let us consider a nonredundant parallel manipulator of m links, n DOF and driven by n actuators. The general Lagrangian dynamic formulation for a nonrigid manipulator can be expressed as [35]

$$\boldsymbol{\tau} = \frac{\mathrm{d}}{\mathrm{dt}}\left(\frac{\partial L}{\partial \dot{\mathbf{q}}_a}\right) - \frac{\partial L}{\partial \mathbf{q}_a} \tag{1a}$$

$$\mathbf{0} = \frac{\mathrm{d}}{\mathrm{dt}}\left(\frac{\partial L}{\partial \dot{\mathbf{q}}_e}\right) - \frac{\partial L}{\partial \mathbf{q}_e} \tag{1b}$$

where,

- L is the Lagrangian of the manipulator; $L = T - V$, where T is the kinetic energy and V is the potential energy due to gravitational forces, friction, and elasticity;
- $\mathbf{q}_a = [q_1^a, q_2^a, ..., q_n^a]^T$ and $\dot{\mathbf{q}}_a = [\dot{q}_1^a, \dot{q}_2^a, ..., \dot{q}_n^a]^T$ represent the vectors of position and velocity of the actuators, respectively;
- $\mathbf{q}_e = [q_1^e, q_2^e, ..., q_n^e]^T$ and $\dot{\mathbf{q}}_e = [\dot{q}_1^e, \dot{q}_2^e, ..., \dot{q}_n^e]^T$ represent the vectors of position and velocity of the elastic coordinates (deformations of links and joints);
- $\boldsymbol{\tau}$ is the vector of the actuators efforts.

In general, for parallel manipulators, the potential and kinetic energies not only explicitly depend both of the actuated variables $\mathbf{q}_a$ and elastic coordinates $\mathbf{q}_e$, but also from the positions $\mathbf{x}$ and velocities $\mathbf{v}$ of the payload. Therefore it is preferable to rewrite Eq. (1) using the Lagrange multipliers [35], as follows:

$$\boldsymbol{\tau} = \mathbf{W_b} + \mathbf{B}^T\boldsymbol{\lambda}, \quad \mathbf{W_b} = \frac{\mathrm{d}}{\mathrm{dt}}\left(\frac{\partial L}{\partial \dot{\mathbf{q}}_a}\right) - \frac{\partial L}{\partial \mathbf{q}_a} \tag{2a}$$

$$\mathbf{0} = \mathbf{W_c} + \mathbf{C}^T\boldsymbol{\lambda}, \quad \mathbf{W_c} = \frac{\mathrm{d}}{\mathrm{dt}}\left(\frac{\partial L}{\partial \dot{\mathbf{q}}_e}\right) - \frac{\partial L}{\partial \mathbf{q}_e} \tag{2b}$$

where $\boldsymbol{\lambda}$ is the Lagrange multipliers vector, which is related to the wrench $\mathbf{W_p}$ applied on the platform by

$$\mathbf{A}^T\boldsymbol{\lambda} = \mathbf{W_p}, \quad \mathbf{W_p} = \left(\frac{\mathrm{d}}{\mathrm{dt}}\left(\frac{\partial L}{\partial \mathbf{v}}\right) - \frac{\partial L}{\partial \mathbf{x}}\right) \tag{3}$$

and

- $\mathbf{x} = [x, y, z, \phi, \psi, \theta]^T$ and $\mathbf{v} = [\dot{x}, \dot{y}, \dot{z}, \dot{\phi}, \dot{\psi}, \dot{\theta}]^T$ are vectors containing the end-effector trajectory parameters and their derivatives, respectively; x, y, z represents the position of the controlled point in the global frame and ϕ, ψ, and θ the rotation of the platform about three axes $\mathbf{a}_\varphi$, $\mathbf{a}_\psi$, and $\mathbf{a}_\theta$. Vector $\mathbf{x}$ depends on both rigid coordinates $\mathbf{q}_a$ and elastic coordinates $\mathbf{q}_e$.
- $\mathbf{A}$, $\mathbf{B}$, and $\mathbf{C}$ are three matrices relating the vectors $\mathbf{v}$, $\dot{\mathbf{q}}_e$, and $\dot{\mathbf{q}}_a$ according to $\mathbf{Av} = \mathbf{B}\dot{\mathbf{q}}_a + \mathbf{C}\dot{\mathbf{q}}_e$. They can be found by differentiating the closure equations $f_i(\mathbf{x},\mathbf{q}_a,\mathbf{q}_e) = 0$ (taking into account the rigid as well as the elastic coordinates [35]) with respect to time. In the hypothesis of small elastic displacements ($\mathbf{q}_e \approx \mathbf{0}$), matrices $\mathbf{A}$ and $\mathbf{B}$ may be found assuming that the robot is composed of rigid links only.
- $\mathbf{W_p}$ is the wrench applied on the platform by the legs and external forces expressed along axes $\mathbf{a}_\varphi$, $\mathbf{a}_\psi$, and $\mathbf{a}_\theta$ [36].

Expressing $\mathbf{W_p}$ in the base frame, one can obtain

$$\boldsymbol{\tau} = \mathbf{W_b} + \mathbf{J}_{\mathbf{q}_a}^{T\,R_0}\mathbf{W_p} \tag{4a}$$

$$\mathbf{0} = \mathbf{W_c} + \mathbf{J}_{\mathbf{q}_e}^{T\,R_0}\mathbf{W_p} \tag{4b}$$

where $\mathbf{J}_{\mathbf{q}_a} = \left({}^{\mathbf{R}_0}\mathbf{A}\right)^{-1}\mathbf{B}$ is the square Jacobian matrix between the twist $\mathbf{t}$ of the platform (expressed in the base frame) and the vector $\dot{\mathbf{q}}_a$ of actuators velocities, $\mathbf{J}_{\mathbf{q}_e} = \left({}^{\mathbf{R}_0}\mathbf{A}\right)^{-1}\mathbf{C}$ is the nonsquare Jacobian matrix between twist $\mathbf{t}$ of the platform (expressed in the base frame) and the vector $\dot{\mathbf{q}}_e$ of deformations velocities, ${}^{\mathbf{R}_0}\mathbf{A} = \mathbf{AD}$ is the expression of matrix $\mathbf{A}$ in the base frame, where $\mathbf{D}$ is a transformation matrix, of which expression is given in Ref. [37].

For any prescribed trajectory $\mathbf{x}(t)$, the values of vector $\mathbf{q}_a$ can be found using the inverse kinematics and dynamics. Thus, taking into account that the manipulator is not in a Type 1 singularity [1], i.e., the mechanism is at a configuration where it loses one DOF, the terms $\mathbf{W_b}$, $\mathbf{W_c}$, and ${}^{\mathbf{R}_0}\mathbf{W_p}$ can be computed [38]. However, for a trajectory passing through a Type 2 singularity, the determinant of matrix ${}^{\mathbf{R}_0}\mathbf{A}$ vanishes. Numerically, the values of the efforts applied by the actuators become infinite. In practice, the manipulator either is locked in such a position of the end-effector or it can not follow the prescribed trajectory.

As it is mentioned above, in a Type 2 singularity, the determinant of matrix ${}^{\mathbf{R}_0}\mathbf{A}$ vanishes. In other words, at least two of its columns are linearly dependant [37]. So, one may obtain such a relationship

$${}^{R_0}\mathbf{A}\,\mathbf{t_s} = \mathbf{0} \Rightarrow \mathbf{t_s}^{T\,R_0}\mathbf{A}^T = \mathbf{0}^T \tag{5}$$

where the vector $\mathbf{t_s}$ represents the direction of the uncontrollable motion of the platform in a Type 2 singularity.

Then, by dot-multiplying both sides of Eq. (3) by $\mathbf{t_s}$ and taking into account Eq. (5), we obtain

$$\mathbf{t}_\mathbf{s}^{T\,R_0}\mathbf{A}^T\boldsymbol{\lambda} = 0 \tag{6}$$

which also implies that

$$\mathbf{t}_\mathbf{s}^{T\,R_0}\mathbf{W_p} = 0 \tag{7}$$

Thus, Eq. (7) corresponds to the scalar product of vectors $\mathbf{t_s}$ and ${}^{\mathbf{R}_0}\mathbf{W_p}$.

Thus, in the presence of a Type 2 singularity, it is possible to satisfy conditions (7) if the wrench applied on the platform by the legs and external efforts ${}^{\mathbf{R}_0}\mathbf{W_p}$ are reciprocal to the direction of the uncontrollable motion $\mathbf{t_s}$. Otherwise, the dynamic model is not consistent. Obviously, in the presence of a Type 2 singularity, the displacement of the end-effector of the manipulator has to be planned to satisfy Eq. (7). Therefore, our task will be to achieve a trajectory which will allow the manipulator passing trough the Type 2 singularities, i.e., which will allow the manipulator respecting condition (7).

Section 3, an example illustrates the obtained results discussed above. This example presents a planar 5*R* flexible parallel manipulator.

3 Illustrative Example

In the planar 5*R* parallel manipulator, as shown in Fig. 1, the output point is connected to the base by two legs, each of which consists of three revolute joints and two links. In each of the two legs, the revolute joint connected to the base is actuated. Thus, such a manipulator is able to position its output point in a plane.

As shown in Fig. 1, the input joints are denoted as A and E. The orientation of elements 1 and 2 are denoted q_1^e and q_2^e, respectively. The common joint of the two legs is denoted as C, which is also the output axis with controlled parameters $\mathbf{x} = [x, y]^T$. A fixed global reference system ***xOy*** is located at the middle of segment

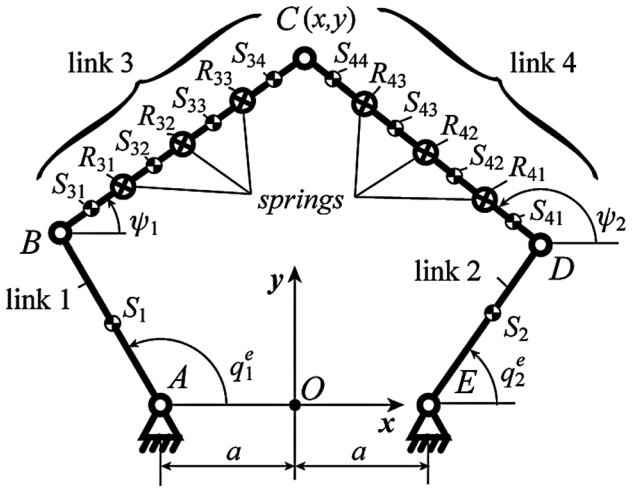

Fig. 1 Kinematic chain of the planar 5*R* parallel manipulator

AE with the *y*-axis normal to *AE* and the *x*-axis directed along *AE*. The lengths of the links (*AB* and *DE*) and (*BC* and *CD*), are respectively, denoted as L_p and L_d.

Actuators 1 and 2 are connected to links 1 and 2, respectively, via Harmonic Drive® systems which are represented by a model similar to that given in Ref. [39]. The position of actuator i is denoted as q_i^a. It is assumed that the actuator i is capable to deliver a couple τ_i to the motor shaft, which is elastically coupled to the link i of the robot ($i=1$ or 2). The flexibility of the drive system is modeled by a torsion spring with stiffness k_1. The gear ratio is denoted n. I_a is the axial moment of inertia of the motor i plus the Harmonic drive system.

The deformations of the robot links 3 and 4 are modeled by adding virtual torsion springs at points R_{ij} ($i=3$, 4 and $j=1$–3), such as elements 3 and 4 are decomposed into four sub-elements, denoted as elements iv ($i=3$, 4 and $v=1$–4), with identical lengths and inertia properties. The stiffness of these springs is denoted as k_2. The displacement of the spring mounted at point R_{ij} will be denoted as ε_{ij}.

The singularity analysis of this manipulator shows that the Type 2 singularities appear when links 3 and 4 are parallel [40] (Fig. 2). In both cases, the gained degree of freedom is an infinitesimal translation perpendicular to the links 3 and 4.

Taking into account that the gravity is directed along z axis (perpendicular to the plane of motions), the expression of the potential energy V may be written as

$$V = 0.5\left(k_1\,(\mathbf{q}_a/n - \mathbf{q}_e)^T(\mathbf{q}_a/n - \mathbf{q}_e) + k_2\,\boldsymbol{\varepsilon}^T\boldsymbol{\varepsilon}\right) \tag{8}$$

where $\mathbf{q}_a = [q_1^a, q_2^a]^T$, $\mathbf{q}_e = [q_1^e, q_2^e]^T$, and $\boldsymbol{\varepsilon} = [\varepsilon_{31},\ \varepsilon_{32},\ \varepsilon_{33},\ \varepsilon_{41},\ \varepsilon_{42},\ \varepsilon_{43}]^T$.

The expression of the kinetic energy is

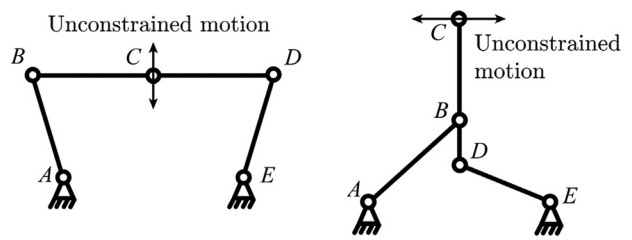

(a) $\psi_1 = \psi_2 \pm \pi$ (b) $\psi_1 = \psi_2$

Fig. 2 Type 2 singular configurations of the planar 5*R* parallel manipulator

$$T = 0.5\Big(I_a\,\dot{\mathbf{q}}_a^T\dot{\mathbf{q}}_a + I_p\,\dot{\mathbf{q}}_e^T\dot{\mathbf{q}}_e + I_d(\dot{\boldsymbol{\psi}}^T\dot{\boldsymbol{\psi}} + (\dot{\boldsymbol{\psi}} + \dot{\boldsymbol{\varepsilon}}_\mathbf{1})^T(\dot{\boldsymbol{\psi}} + \dot{\boldsymbol{\varepsilon}}_\mathbf{1}) + (\dot{\boldsymbol{\psi}} + \dot{\boldsymbol{\varepsilon}}_\mathbf{1} + \dot{\boldsymbol{\varepsilon}}_\mathbf{2})^T(\dot{\boldsymbol{\psi}} + \dot{\boldsymbol{\varepsilon}}_\mathbf{1} + \dot{\boldsymbol{\varepsilon}}_\mathbf{2}) + (\dot{\boldsymbol{\psi}} + \dot{\boldsymbol{\varepsilon}}_\mathbf{1} + \dot{\boldsymbol{\varepsilon}}_\mathbf{2} + \dot{\boldsymbol{\varepsilon}}_\mathbf{3})^T \times (\dot{\boldsymbol{\psi}} + \dot{\boldsymbol{\varepsilon}}_\mathbf{1} + \dot{\boldsymbol{\varepsilon}}_\mathbf{2} + \dot{\boldsymbol{\varepsilon}}_\mathbf{3})) + m_p\sum_{i=1}^{2}\mathbf{v}_{Si}^T\mathbf{v}_{Si} + m_d\sum_{i=3}^{4}\sum_{j=1}^{4}\mathbf{v}_{Sij}^T\mathbf{v}_{Sij}\Big) \tag{9}$$

where

- $\dot{\boldsymbol{\psi}} = [\dot{\psi}_1, \dot{\psi}_2]^T$ is the vector of the angular velocities of elements 3 and 4,
- $\dot{\boldsymbol{\varepsilon}}_j = [\dot{\varepsilon}_{3j}, \dot{\varepsilon}_{4j}]^T$, $j=1$–3
- $\mathbf{v}_{Si}$ is the translational velocity vector of the center of masses of element i ($i=1$,2); the center of masses is located at the middle of the considered segment.
- $\mathbf{v}_{Sij}$ is the translational velocity vector of the center of masses of element ij ($i=3$,4 and $j=1$–3); the center of masses is located at the middle of the considered segment.
- m_p is the mass of the proximal links (elements 1 and 2), m_d is the mass of each sub-elements of the distal links (elements ij, ($i=3$,4 and $j=1$–4));
- I_p is the axial moment of inertia of the proximal links (elements 1 and 2), I_d is the axial moment of inertia of each sub-elements of the distal links;

The expressions of vectors $\mathbf{v}_{Si}$ are

$$\mathbf{v}_{Si} = 0.5\,L_p\,\dot{q}_i^e\begin{bmatrix}-\sin q_i^e\\ \cos q_i^e\end{bmatrix},\quad \text{for } i=1,2 \tag{10a}$$

$$\mathbf{v}_{Sij} = L_p\,\dot{q}_i^e\begin{bmatrix}-\sin q_i^e\\ \cos q_i^e\end{bmatrix} + \frac{L_d}{8}\,\dot{\psi}_i\begin{bmatrix}-\sin\psi_i\\ \cos\psi_i\end{bmatrix}\quad \text{for } i=1,2 \text{ and } j=1 \tag{10b}$$

$$\mathbf{v}_{Sij} = \mathbf{v}_{Si(j-1)} + \frac{L_d}{8}\dot{\psi}_i\begin{bmatrix}-\sin\psi_i\\ \cos\psi_i\end{bmatrix} + \frac{L_d}{8}\,(\dot{\psi}_i + \dot{\varepsilon}_{i(j-1)}) \times \begin{bmatrix}-\sin(\psi_i + \varepsilon_{i(j-1)})\\ \cos(\psi_i + \varepsilon_{i(j-1)})\end{bmatrix},\quad \text{for } i=1,2 \text{ and } j=2 \tag{10c}$$

$$\mathbf{v}_{Sij} = \mathbf{v}_{Si(j-1)} + \frac{L_d}{8}(\dot{\psi}_i + \dot{\varepsilon}_{i(j-2)})\begin{bmatrix}-\sin(\psi_i + \varepsilon_{i(j-2)})\\ \cos(\psi_i + \varepsilon_{i(j-2)})\end{bmatrix} + \frac{L_d}{8}\,(\dot{\psi}_i + \dot{\varepsilon}_{i(j-2)} + \dot{\varepsilon}_{i(j-1)})\begin{bmatrix}-\sin(\psi_i + \varepsilon_{i(j-2)} + \varepsilon_{i(j-1)})\\ \cos(\psi_i + \varepsilon_{i(j-2)} + \varepsilon_{i(j-1)})\end{bmatrix}$$
$$\text{for } i=1,2 \text{ and } j=3 \tag{10d}$$

$$\mathbf{v}_{Sij} = \mathbf{v}_{Si(j-1)} + \frac{L_d}{8}(\dot{\psi}_i + \dot{\varepsilon}_{i(j-3)} + \dot{\varepsilon}_{i(j-2)}) \times \begin{bmatrix}-\sin(\psi_i + \varepsilon_{i(j-3)} + \varepsilon_{i(j-2)})\\ \cos(\psi_i + \varepsilon_{i(j-3)} + \varepsilon_{i(j-2)})\end{bmatrix} + \frac{L_d}{8}\,(\dot{\psi}_i + \dot{\varepsilon}_{i(j-3)} + \dot{\varepsilon}_{i(j-2)} + \dot{\varepsilon}_{i(j-1)})\begin{bmatrix}-\sin(\psi_i + \varepsilon_{i(j-3)} + \varepsilon_{i(j-2)} + \varepsilon_{i(j-1)})\\ \cos(\psi_i + \varepsilon_{i(j-3)} + \varepsilon_{i(j-2)} + \varepsilon_{i(j-1)})\end{bmatrix}$$
$$\text{for } i=1,2 \text{ and } j=4 \tag{10e}$$

Introducing Eqs. (10*a*)–(10*e*) into Eq. (9), the dynamic model can be obtained from Eqs. (2) and (3)

$$\mathbf{W}_\boldsymbol{\varepsilon} + \mathbf{J}_\boldsymbol{\varepsilon}^T\mathbf{W}_\mathbf{p} + k_2\boldsymbol{\varepsilon} = \mathbf{0} \tag{11}$$

$$\mathbf{W}_{\mathbf{q}_e} + \mathbf{J}_{\mathbf{q}_e}^T\mathbf{W}_\mathbf{p} - k_1(\mathbf{q}_a/n - \mathbf{q}_e) = \mathbf{0} \tag{12}$$

and

$$\boldsymbol{\tau} = I^a\ddot{\mathbf{q}}_a - k_1(\mathbf{q}_e - \mathbf{q}_a/n)/n \tag{13}$$

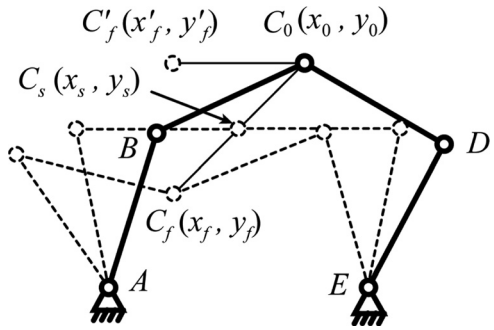

Fig. 3 Initial, singular and final positions of the planar 5*R* parallel manipulator

The terms that appear in this model are described in the appendix.

For given trajectory $\mathbf{x}(t)$, the deformations $\boldsymbol{\varepsilon}(t)$ may de deduced from Eq. (11). However, this equations is difficult to solve analytically, therefore an iterative resolution of the system is used [38]. Once $\boldsymbol{\varepsilon}(t)$ is known, the displacements, velocities, accelerations and other time derivatives of the passive and active variables $\mathbf{q}_e$ and $\boldsymbol{\psi}$ may be found using the dynamic model equations and the loop closure equations, which are given in the appendix. Then, from Eq. (12), the values of $\mathbf{q}_a$ are found

$$\mathbf{q}_a = n\,(\mathbf{W}_{\mathbf{q}_e} + \mathbf{J}_{\mathbf{q}_e}^T \mathbf{W}_\mathbf{p})/k_1 + n\mathbf{q}_e \tag{14}$$

Finally, the input torques $\boldsymbol{\tau}$ can be computed using Eq. (13).

From Eq. (11), it appears that the deformations $\boldsymbol{\varepsilon}$ depends on the position $\mathbf{x}$, velocity $\dot{\mathbf{x}}$ and acceleration $\ddot{\mathbf{x}}$ of the end-effector. As a result, $\ddot{\boldsymbol{\varepsilon}}$ depends on the end-effector position $\mathbf{x}$, velocity $\dot{\mathbf{x}}$, acceleration $\ddot{\mathbf{x}}$, jerk $\dddot{\mathbf{x}}$ and its first derivative $\mathbf{x}^{(4)}$. Thus, $\mathbf{q}_a$ also depends on the same parameters. As a result, from Eq. (13), it can be shown that the input torques depends on the end-effector position, velocity, acceleration, jerk and its first, second and third derivatives with respect to time. Therefore, a 13 deg polynomial has to be applied as a control law when the end-effector is not in the singular configuration.

In order to avoid infinite values of the input torques when crossing a Type 2 singularity, Eq. (7) has to be satisfied. From matrix $\mathbf{A}$ (see appendix), one can find that the twist of the infinitesimal displacement in the singularity can be written under the form

$$\mathbf{t_s} = [-\sin\psi_1, \cos\psi_1]^T \tag{15}$$

Thus, the examined manipulator can pass through the given singular positions if the wrench $\mathbf{W_p}$ determined by Eq. (14) is reciprocal to the direction of the uncontrollable motion $\mathbf{t_s}$ described by Eq. (15). However, the difficulty remains into the fact that, introducing $\mathbf{W_p}$ (see appendix) into Eq. (7) leads to a condition, which depends not only on the end-effector position, velocity and acceleration but also of variables $\boldsymbol{\varepsilon}$, $\dot{\boldsymbol{\varepsilon}}$, and $\ddot{\boldsymbol{\varepsilon}}$, which at any computation step can only be iteratively found. Therefore, contrary to our previous papers [32,34] in which the polynomial laws able to achieve condition (7) were defined analytically, in this case, this law can only be found by using numerical simulation algorithms. An example of the use of such algorithm is given below.

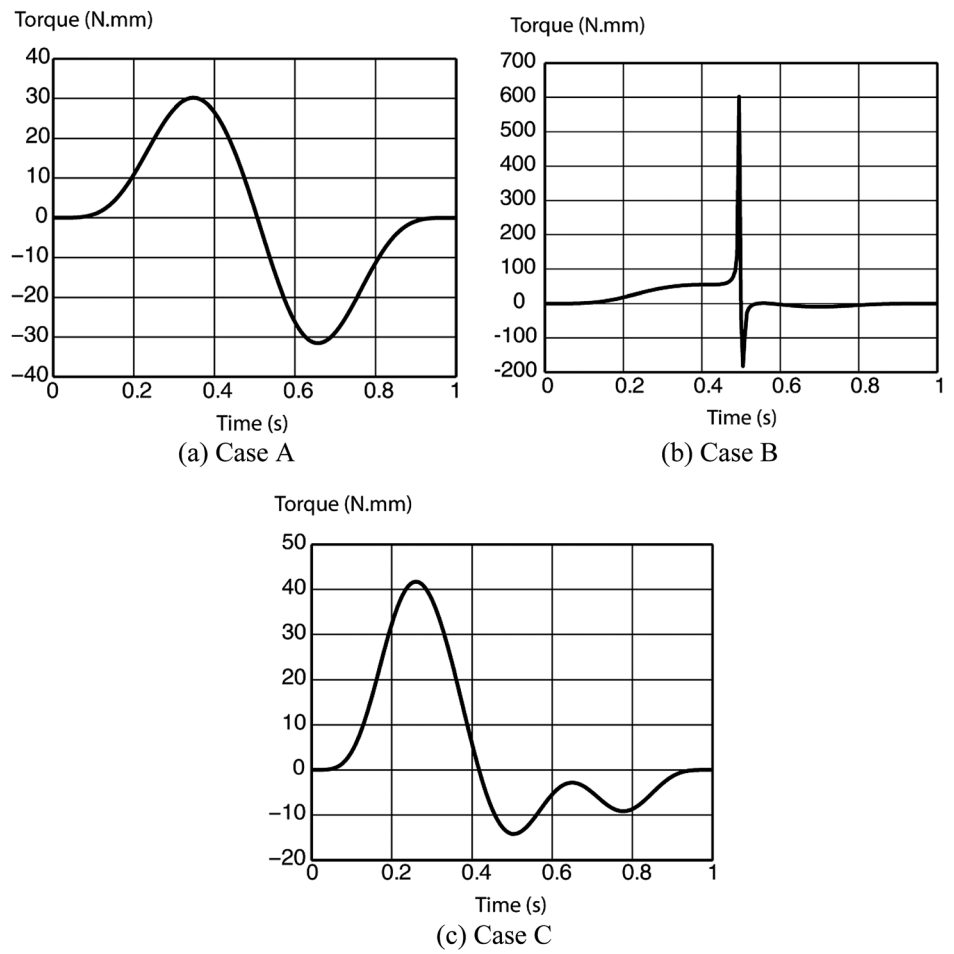

Fig. 4 Torques values for the actuator 1

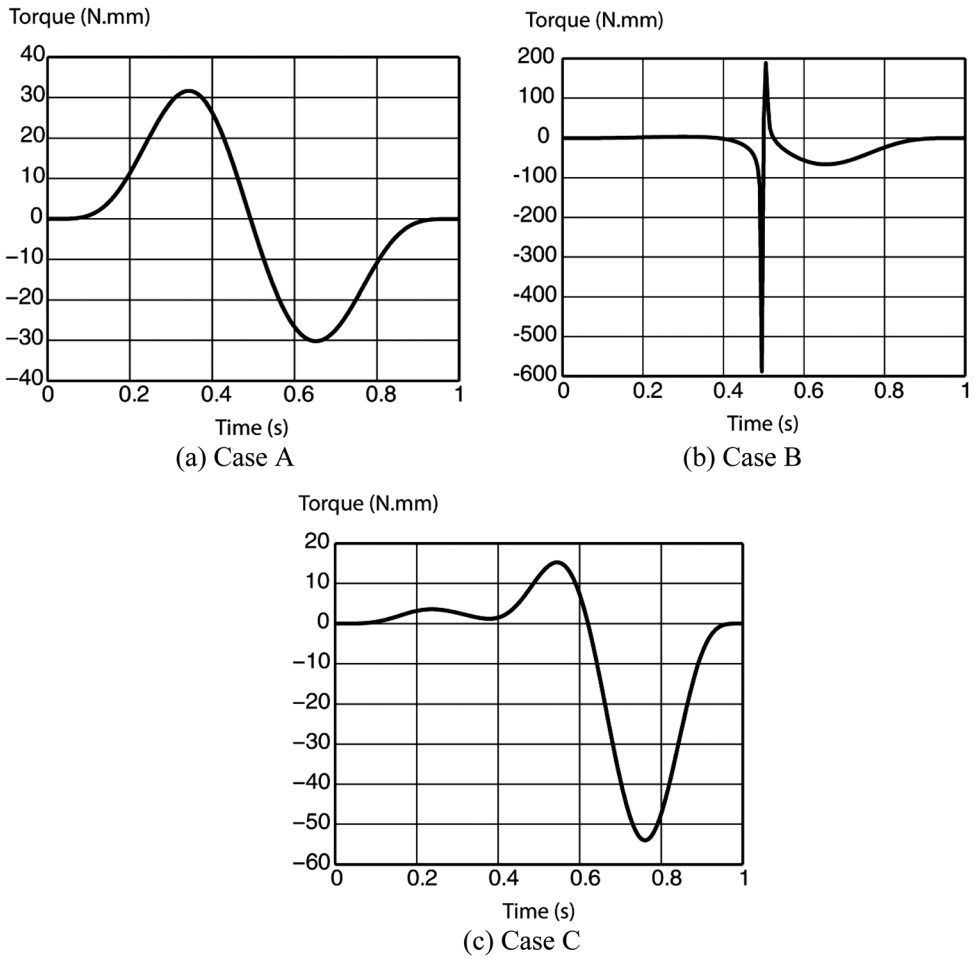

Fig. 5 Torques values for the actuator 2

Let us now determine the trajectory, which makes it possible to satisfy condition (7) for the manipulator with following parameters of links: $a = 0.2$ m, $L_p = L_d = 0.25$ m, $m_p = 1.75$ kg, $m_d = 1.8$ kg, $I_p = 1.18 \times 10^{-2}$ kg m^2, $I_d = 1.5 \times 10^{-4}$ kg m^2, $I_a = 0.064 \times 10^{-4}$ kg m^2, $k_1 = k_2 = 800$ Nm/rad, and $n = 50$.

With regard to the prescribed trajectory generation, the point C should reproduce a motion along a straight line between the initial position $C_0(x_0,y_0) = C_0(0.1,0.345)$ and the final point C_f $(x_f, y_f) = C_f$ (–0.1,0.145) in $t_f = 1$ s (Fig. 3). However, the manipulator will pass by a Type 2 singular position at point $C_s(x_s,y_s) = C_s(0,0.245)$ (Fig. 3).

The trajectory can be expressed as follows

$$\mathbf{x} = \begin{bmatrix} x(t) \\ y(t) \end{bmatrix} = \begin{bmatrix} x_0 + s(t)(x_f - x_0) \\ y_0 + s(t)(y_f - y_0) \end{bmatrix} \tag{16}$$

where $s(t)$ is a polynomial, which should respect the following conditions:

$$s(t_0) = 0 \tag{17}$$

$$s(t_f) = 1 \tag{18}$$

$$\dot{s}(t_0) = \dot{s}(t_f) = 0 \tag{19}$$

$$\ddot{s}(t_0) = \ddot{s}(t_f) = 0 \tag{20}$$

$$\dddot{s}(t_0) = (t_f) = 0 \tag{21}$$

$$d(\dddot{s}(t_0))/dt = d(\dddot{s}(t_f))/dt = 0 \tag{22}$$

$$d^2(\dddot{s}(t_0))/dt^2 = d^2(\dddot{s}(t_f))/dt^2 = 0 \tag{23}$$

$$d^3(\dddot{s}(t_0))/dt^3 = d^3(\dddot{s}(t_f))/dt^3 = 0 \tag{24}$$

$$s(t_s = 0.5\,\text{s}) = 0.5 \tag{25}$$

$$\dot{s}(t_s) > 0 \tag{26}$$

and

$$\mathbf{t}_s^T \mathbf{W}_\mathbf{p} = 0 \tag{27}$$

There are 17 conditions, therefore $s(t)$ should be at least a 16 deg polynomial.

Boundary conditions (17)–(26) are directly linked to the expression of the polynomial, whereas Eq. (27) involve the computation of the entire dynamic model, therefore, one way to find the polynomial is to express conditions (17)–(27) as the following optimization problem

$$f(\mathbf{a}) = \left|\mathbf{t}_s^T \mathbf{W}_\mathbf{p}\right| \rightarrow \min_{\mathbf{a}} \tag{28}$$

subject to constraints (17)–(26), where $\mathbf{a}$ is a vector regrouping the coefficients of the polynomial $s(t)$. It is obvious that such formulation does not imply a 100% guaranty that the function $f(\mathbf{a})$ will be null at the end of the optimization step. However, in general, the simulations have shown that, even if the minimization problem Eq. (28) may not yield a zero result, it was possible to obtain a value close to zero.

A way to solve this problem is to use the goal attainment programming (function "fgoalattain" in MATLAB). The goal attainment optimization allows generating specific Pareto-optimal solutions.

Let us apply the goal-attainment technique that yields the following nonlinear programming formulation:

$$\lambda \rightarrow \min_{\lambda,\mathbf{a}} \tag{29}$$

subject to

$$f(\mathbf{a}) - w_i\lambda \leq f_i^0; \quad h_i(\mathbf{a}) \geq h_i^0; \quad \forall i \tag{30}$$

where $h_i(\mathbf{a}) \geq h_i^0$ represents the constraints (17)–(26). Here, λ is unrestricted scalar variable, $w_i \geq 0$ are designer selected weighting coefficients, and f_i^0 are the goal to be realized for each design objective. In this formulation, minimization of λ tends to force the specifications to meet their goal. If at the solution point, λ is negative, the goals have been over-attained; if λ is positive, then the goals have been under-attained. The method is appealing since it is possible for the user to specify unrealizable objectives and still obtain a solution which represents a compromise. More detailed information about the goal-attainment optimization can be found in Ref. [41].

Using the "fgoalattain" function in MATLAB, with specified constraints (17)–(26) and objective (28), the following polynomial has been found:

$$\begin{aligned} s(t) = {} & 7099.0\,t^7 - 52152.8\,t^8 + 160698.1\,t^9 - 252912.5\,t^{10} \\ & + 173271.6\,t^{11} + 60944.0t^{12} - 217870.6\,t^{13} + 179095.5\,t^{14} \\ & - 68776.9\,t^{15} + 10605.7\,t^{16} \end{aligned} \tag{31}$$

This polynomial will be implemented into the dynamic model of the manipulator in order to verify that it allows the passing through the Type 2 singularity. The simulations have been carried out using the software ADAMS.

In order to compare the different cases of trajectory planning, in Figs. 4 and 5 are given the values of the input torques obtained using the software ADAMS for the following numerical simulations:

A: a trajectory between points C_0 and C'_f $(x'_f,\ y'_f) = C'_f$ $(-0.1,345)$ (Fig. 3) without meeting any singularity. For such a case, a thirteenth order polynomial law has been defined from conditions (17)–(24). The obtained $s(t) = 1716\,t^7 - 9009\,t^8 + 20020\,t^9 - 24024\,t^{10} + 16380t^{11}$ $-6006\,t^{12} + 924\,t^{13}$ polynomial law is used for the trajectory planning out of the singular zone of the manipulator. In this case the values of the input torques are finite.

B: the same thirteenth order polynomial law $s(t) = 1716\,t^7 - 9009\,t^8 + 20020\,t^9 - 24024\,t^{10} + 16380t^{11} - 6006\,t^{12} + 924\,t^{13}$ is used for the trajectory planning between C_0 and C_f inside the singular zone of the manipulator. In this case the values of the input torques close to the singular positions tend to infinity.

C: the sixteenth order polynomial law of Eq. (31) for the trajectory planning of the manipulator inside the singular zone. The obtained results show that the values of the input torques are finite.

It is interesting to observe the manipulator's behavior for the simulated cases. The first law, which is a thirteenth order polynomial, assumes the prescribed motion without perturbation of torques outside of the singular zone. The same law does not provide the stable motion in the presence of singularity. The sixteenth order polynomial law reestablishes the stable motion for passing through the singular position.

4 Conclusion

In our previous work, we have shown that any parallel manipulator can pass through the singular positions without perturbation of motion if the wrench applied on the end-effector by the legs and external efforts is reciprocal to the twist along the direction of the uncontrollable motion [32]. This condition was applied to the rigid-link manipulators. The obtained results showed that the planning of motion for assuming the optimal force generation can be carried out by an eight order polynomial law. In Ref. [34] the rigid-link flexible-joint manipulators have been studied. It was shown that the degree of the polynomial law should be different, when the flexibility of actuated joints is introduced. The obtained results disclosed that the planning of motion for assuming the optimal force generation in the rigid-link flexible-joint manipulators must be carried out by a twelfth order polynomial law.

In this paper, we have expanded the information about the dynamic properties of parallel manipulators in the presence of Type 2 singularity by including in the studied problem the link flexibility. The obtained results have shown that the planning of motion for assuming the optimal force generation in the manipulators with flexible links must be now carried out by a sixteenth order polynomial law.

The suggested technique was illustrated by a 5*R* planar parallel manipulator. The obtained results have been validated by numerical simulations carried out using the software ADAMS.

Appendix

From Eqs. (2) and (3), vectors $\mathbf{W}_{\boldsymbol{\varepsilon}}$, $\mathbf{W}_{\mathbf{q}_e}$, and $\mathbf{W}_{\mathbf{p}}$ can be found

$$\mathbf{W}_{\mathbf{p}} = \frac{d}{dt}\left(\frac{\partial L}{\partial \mathbf{v}}\right) - \frac{\partial L}{\partial \mathbf{x}} = \left(\mathbf{J}_{\mathbf{x}\psi}^T + \mathbf{J}_{\boldsymbol{\varepsilon}}^{-T}\mathbf{J}_{\boldsymbol{\varepsilon}\psi}^T + \mathbf{J}_{\mathbf{q}_e}^{-T}\mathbf{J}_{\mathbf{q}_e\psi}^T\right)\mathbf{W}_{\boldsymbol{\psi}} \tag{A1}$$

$$\mathbf{W}_{\mathbf{q}_e} = \frac{d}{dt}\left(\frac{\partial L}{\partial \dot{\mathbf{q}}_e}\right) - \frac{\partial L}{\partial \mathbf{q}_e} = \left(I_p + m_p l_p^2\right)\ddot{\mathbf{q}}_e + m_d\mathbf{F}_{\mathbf{q}_e} \tag{A2}$$

$$\mathbf{W}_{\boldsymbol{\varepsilon}} = \frac{d}{dt}\left(\frac{\partial L}{\partial \dot{\boldsymbol{\varepsilon}}}\right) - \frac{\partial L}{\partial \boldsymbol{\varepsilon}} = I_d\mathbf{E} + m_d\mathbf{F}_{\boldsymbol{\varepsilon}} \tag{A3}$$

with

$$\mathbf{W}_{\boldsymbol{\psi}} = I_d\left(4\ddot{\boldsymbol{\psi}} + \ddot{\boldsymbol{\varepsilon}}_{\mathbf{1}} + \ddot{\boldsymbol{\varepsilon}}_{\mathbf{2}} + \ddot{\boldsymbol{\varepsilon}}_{\mathbf{3}} + \ddot{\boldsymbol{\varepsilon}}_{\mathbf{4}}\right) + m_d\mathbf{F}_{\boldsymbol{\psi}} \tag{A4}$$

$$\mathbf{E} = [e_{11}, e_{12}, e_{13}, e_{21}, e_{22}, e_{23}]^T \tag{A5}$$

where for $i = 3, 4$

$$e_{i1} = 3\,\ddot{\psi}_i + 3\ddot{\varepsilon}_{i1} + 2\ddot{\varepsilon}_{i2} + \ddot{\varepsilon}_{i3} \tag{A6a}$$

$$e_{i2} = 2\,\ddot{\psi}_i + 2\ddot{\varepsilon}_{i2} + \ddot{\varepsilon}_{i3} \tag{A6b}$$

$$e_{i3} = \ddot{\psi}_i + \ddot{\varepsilon}_{i3} \tag{A6c}$$

$$\mathbf{F}_{\boldsymbol{\psi}} = \frac{d}{dt}\left(\frac{\partial f}{\partial \dot{\boldsymbol{\psi}}}\right) - \frac{\partial f}{\partial \boldsymbol{\psi}}, \quad f = \sum_{i=3}^{4}\sum_{j=1}^{4}\mathbf{v}_{Sij}^T\mathbf{v}_{Sij} \tag{A7}$$

$$\mathbf{F}_{\mathbf{q}_e} = \frac{d}{dt}\left(\frac{\partial f}{\partial \dot{\mathbf{q}}_e}\right) - \frac{\partial f}{\partial \mathbf{q}_e} \tag{A8}$$

$$\mathbf{F}_{\boldsymbol{\varepsilon}} = \frac{d}{dt}\left(\frac{\partial f}{\partial \dot{\boldsymbol{\varepsilon}}}\right) - \frac{\partial f}{\partial \boldsymbol{\varepsilon}} \tag{A9}$$

Matrices $\mathbf{J}_{\boldsymbol{\varepsilon}}$ and $\mathbf{J}_{\mathbf{q}e}$, of Eqs. (11)–(13) may be found from the loop closure equations between $\mathbf{x}$, $\boldsymbol{\varepsilon}$, and $\mathbf{q}_e$:

$$\begin{aligned} f_1 = {} & (x + a - L_p\cos q_1^e)^2 + (y - L_p\sin q_1^e)^2 - L_d^2(2 + \cos\varepsilon_{11} \\ & + \cos(\varepsilon_{11} + \varepsilon_{12}) + \cos(\varepsilon_{11} + \varepsilon_{12} + \varepsilon_{13}) + \cos(2\varepsilon_{11} + \varepsilon_{12}) \\ & + \cos(2\varepsilon_{11} + \varepsilon_{12} + \varepsilon_{13}) + \cos(2\varepsilon_{11} + 2\varepsilon_{12} + \varepsilon_{13}))/8 = 0 \end{aligned} \tag{A10a}$$

$$\begin{aligned} f_2 = {} & (x - a - L_p\cos q_2^e)^2 + (y - L_p\sin q_2^e)^2 - L_d^2(2 + \cos\varepsilon_{21} \\ & + \cos(\varepsilon_{21} + \varepsilon_{22}) + \cos(\varepsilon_{21} + \varepsilon_{22} + \varepsilon_{23}) + \cos(2\varepsilon_{21} + \varepsilon_{22}) \\ & + \cos(2\varepsilon_{21} + \varepsilon_{22} + \varepsilon_{23}) + \cos(2\varepsilon_{21} + 2\varepsilon_{22} + \varepsilon_{23}))/8 = 0 \end{aligned} \tag{A10b}$$

from which it comes

$$\mathbf{A}=\left[\frac{\partial f_i}{\partial \mathbf{x}}\right]=\begin{bmatrix} a_{11} & a_{12} \\ a_{21} & a_{22} \end{bmatrix}=2\begin{bmatrix} x-L_p\cos q_1^e+a & y-L_p\sin q_1^e \\ x-L_p\cos q_2^e-a & y-L_p\sin q_2^e \end{bmatrix} \tag{A11}$$

$$\mathbf{B}=\left[\frac{\partial f_i}{\partial \mathbf{q}_e}\right]=-L_p\begin{bmatrix} a_{12}\cos q_1^e-a_{11}\sin q_1^e & 0 \\ 0 & a_{22}\cos q_2^e-a_{21}\sin q_2^e \end{bmatrix} \tag{A12}$$

$$\mathbf{C}=\left[\frac{\partial f_i}{\partial \boldsymbol{\varepsilon}}\right]=\frac{L_d}{8}\begin{bmatrix} c_{11} & c_{12} & c_{13} & 0 & 0 & 0 \\ 0 & 0 & 0 & c_{24} & c_{25} & c_{26} \end{bmatrix}\approx \mathbf{0} \tag{A13}$$

with, for $i=1, 2$

$$\begin{aligned} c_{i1}=&\sin\varepsilon_{i1}+\sin(\varepsilon_{i1}+\varepsilon_{i2})+\sin(\varepsilon_{i1}+\varepsilon_{i2}+\varepsilon_{i3})+2\sin(2\varepsilon_{i1}+\varepsilon_{i2})\\ &+2\sin(2\varepsilon_{i1}+\varepsilon_{i2}+\varepsilon_{i3})+2\sin(2\varepsilon_{i1}+2\varepsilon_{i2}+\varepsilon_{i3}) \end{aligned} \tag{A14a}$$

$$\begin{aligned} c_{i2}=&\sin(\varepsilon_{i1}+\varepsilon_{i2})+\sin(\varepsilon_{i1}+\varepsilon_{i2}+\varepsilon_{i3})+\sin(2\varepsilon_{i1}+\varepsilon_{i2})\\ &+\sin(2\varepsilon_{i1}+\varepsilon_{i2}+\varepsilon_{i3})+2\sin(2\varepsilon_{i1}+2\varepsilon_{i2}+\varepsilon_{i3}) \end{aligned} \tag{A14b}$$

$$\begin{aligned} c_{i3}=&\sin(\varepsilon_{i1}+\varepsilon_{i2}+\varepsilon_{i3})+\sin(2\varepsilon_{i1}+\varepsilon_{i2}+\varepsilon_{i3})\\ &+\sin(2\varepsilon_{i1}+2\varepsilon_{i2}+\varepsilon_{i3}) \end{aligned} \tag{A14c}$$

As a result, it can be found that

$$\mathbf{v}=-\mathbf{A}^{-1}(\mathbf{B}\dot{\mathbf{q}}_e+\mathbf{C}\dot{\varepsilon})=\mathbf{J}_{\mathbf{q}e}\dot{\mathbf{q}}_e+\mathbf{J}_{\varepsilon}\dot{\boldsymbol{\varepsilon}} \tag{A15}$$

and also that

$$\begin{aligned} \dot{\mathbf{q}}_e&=-\mathbf{B}^{-1}(\mathbf{A}\mathbf{v}+\mathbf{C}\ddot{\varepsilon}),\\ \ddot{\mathbf{q}}_e&=-\mathbf{B}^{-1}(\mathbf{A}\dot{\mathbf{v}}+\dot{\mathbf{A}}\mathbf{v}+\mathbf{C}\ddot{\boldsymbol{\varepsilon}}+\dot{\mathbf{C}}\dot{\boldsymbol{\varepsilon}}+\dot{\mathbf{B}}\dot{\mathbf{q}}_e) \end{aligned} \tag{A16}$$

Matrices $\mathbf{J}_{\mathbf{x}\psi}^T$, $\mathbf{J}_{\varepsilon\psi}^T$, and $\mathbf{J}_{\mathbf{q}_e\psi}^T$ of Eq. (A1) may be found from loop closure equations between $\mathbf{x}$, $\mathbf{q}_e$, $\boldsymbol{\varepsilon}$, and $\boldsymbol{\psi}$:

$$\begin{aligned} g_1=&x+a-L_p\cos q_1^e-L_d(\cos\psi_1+\cos(\psi_1+\varepsilon_{11})\\ &+\cos(\psi_1+\varepsilon_{11}+\varepsilon_{12})+\cos(\psi_1+\varepsilon_{11}+\varepsilon_{12}+\varepsilon_{13}))/4=0 \end{aligned} \tag{A17a}$$

$$\begin{aligned} g_2=&x-a-L_p\cos q_2^e-L_d(\cos\psi_2+\cos(\psi_2+\varepsilon_{21})\\ &+\cos(\psi_2+\varepsilon_{21}+\varepsilon_{22})+\cos(\psi_2+\varepsilon_{21}+\varepsilon_{22}+\varepsilon_{23}))/4=0 \end{aligned} \tag{A17b}$$

$$\begin{aligned} g_3=&y-L_p\sin q_1^e-L_d(\sin\psi_1+\sin(\psi_1+\varepsilon_{11})\\ &+\sin(\psi_1+\varepsilon_{11}+\varepsilon_{12})+\sin(\psi_1+\varepsilon_{11}+\varepsilon_{12}+\varepsilon_{13}))/4=0 \end{aligned} \tag{A17c}$$

$$\begin{aligned} g_4=&y-L_p\sin q_2^e-L_d(\sin\psi_2+\sin(\psi_2+\varepsilon_{21})\\ &+\sin(\psi_2+\varepsilon_{21}+\varepsilon_{22})+\sin(\psi_2+\varepsilon_{21}+\varepsilon_{22}+\varepsilon_{23}))/4=0 \end{aligned} \tag{A17d}$$

from which it comes

$$\mathbf{A}_{\psi}=\left[\frac{\partial g_i}{\partial \mathbf{x}}\right]=\begin{bmatrix} 1 & 0 \\ 1 & 0 \\ 0 & 1 \\ 0 & 1 \end{bmatrix} \tag{A18}$$

$$\mathbf{B}_{\psi}=-\left[\frac{\partial g_i}{\partial \mathbf{q}_e}\right]=-L_p\begin{bmatrix} -\sin q_1^e & 0 \\ 0 & -\sin q_2^e \\ \cos q_1^e & 0 \\ 0 & \cos q_2^e \end{bmatrix} \tag{A19}$$

$$\mathbf{C}_{\psi}=\left[\frac{\partial g_i}{\partial \boldsymbol{\varepsilon}}\right]=-\frac{L_d}{4}\begin{bmatrix} -3\sin\psi_1 & -2\sin\psi_1 & -\sin\psi_1 & 0 & 0 & 0 \\ 0 & 0 & 0 & -3\sin\psi_2 & -2\sin\psi_2 & -\sin\psi_2 \\ 3\cos\psi_1 & 2\cos\psi_1 & \cos\psi_1 & 0 & 0 & 0 \\ 0 & 0 & 0 & 3\cos\psi_2 & 2\cos\psi_2 & \cos\psi_2 \end{bmatrix} \tag{A20}$$

$$D_{\psi}=\left[\frac{\partial g_i}{\partial \boldsymbol{\varepsilon}}\right]=-L_d\begin{bmatrix} -\sin\psi_1 & 0 \\ 0 & -\sin\psi_2 \\ \cos\psi_1 & 0 \\ 0 & \cos\psi_2 \end{bmatrix} \tag{A21}$$

As a result, it can be found that

$$\begin{aligned} \dot{\boldsymbol{\psi}}&=-(\mathbf{D}_{\psi}^T\mathbf{D}_{\psi})^{-1}\mathbf{D}_{\psi}^T(\mathbf{A}_{\psi}\mathbf{v}+\mathbf{B}_{\psi}\dot{\mathbf{q}}_e+\mathbf{C}_{\psi}\dot{\boldsymbol{\varepsilon}})\\ &=\mathbf{J}_{\mathbf{x}\psi}\mathbf{v}+\mathbf{J}_{\mathbf{q}_e\psi}\dot{\mathbf{q}}_e+\mathbf{J}_{\varepsilon\psi}\dot{\boldsymbol{\varepsilon}} \end{aligned} \tag{A22}$$

and

$$\begin{aligned} \ddot{\boldsymbol{\psi}}=&-(\mathbf{D}_{\psi}^T\mathbf{D}_{\psi})^{-1}\mathbf{D}_{\psi}^T(\mathbf{A}_{\psi}\dot{\mathbf{v}}+\mathbf{B}_{\psi}\ddot{\mathbf{q}}_e+\mathbf{C}_{\psi}\ddot{\boldsymbol{\varepsilon}}+\dot{\mathbf{A}}_{\psi}\mathbf{v}+\dot{\mathbf{B}}_{\psi}\dot{\mathbf{q}}_e\\ &+\dot{\mathbf{C}}_{\psi}\dot{\boldsymbol{\varepsilon}}+\dot{\mathbf{D}}_{\psi}\dot{\boldsymbol{\psi}}) \end{aligned} \tag{A23}$$

References

[1] Gosselin, C. M., and Angeles, J., 1990, "Singularity Analysis of Closed-Loop Kinematic Chains," IEEE Trans. Rob. Autom., **6**(3), pp. 281–290.

[2] Zlatanov, D., Fenton, R. G., and Benhabib, B., 2010, "Singularity Analysis of Mechanisms and Robots via a Velocity-Equation Model of the Instantaneous Kinematics," *Proceedings of the 1994 IEEE International Conference on Robotics and Automation*, pp. 980–991.

[3] Zein, M., Wenger, P., and Chablat, D., 2007, "Singular Curves in the Joint Space and Cusp Points of 3-RPR Parallel Manipulators," Robotica, **25**(6) pp. 717–724.

[4] Zein, M., Wenger, P., and Chablat, D., 2008, "Non-Singular Assembly-mode Changing Motions for 3-RPR Parallel Manipulators," Mech. Mach. Theory, **43**(4), pp. 480–490.

[5] Kanaan, D., Wenger, P., Caro, S., and Chablat, D., 2009, "Singularity Analysis of Lower-Mobility Parallel Manipulators Using Grassmann-Cayley Algebra," IEEE Trans. Rob. Autom., **25**(5), pp. 995–1004.

[6] Zlatanov, D., Bonev, I. A., and Gosselin, C. M., 2002, Constraint Singularities of Parallel Mechanisms," IEEE International Conference on Robotics and Automation (ICRA 2002), Washington, D. C., May 11–15.

[7] Hunt, K. H., 1987, "Special Configurations of Robot-Arms via Screw Theory," Robotica, **5**, pp. 17–22.

[8] Merlet, J.-P., 1989, "Singular Configurations of Parallel Manipulators and Grassmann Geometry," Int. J. Robot. Res., **8**(5), pp. 45–56.

[9] Bonev, I. A., Zlatanov, D., and Gosselin, C. M., 2003, "Singularity Analysis of 3-DOF Planar Parallel Mechanisms via Screw Theory," ASME J. Mech. Des., **125**(3), pp. 573–581.

[10] Husty, M., and Gosselin, C. M., 2008, "On the Singularity Surface of Planar 3-RPR Parallel Mechanisms," *MUSME 2008 Symposium*, San Juan, Argentine, Vol. **36**(4), pp. 411–425.

[11] Bandyopadhyay, S., and Ghosal, A., 2004, "Analysis of Configuration Space Singularities of Closed-Loop Mechanisms and Parallel Manipulators," Mech. Mach. Theory, **39**(5), pp. 519–544.

[12] Briot, S., Bonev, I. A., Chablat, D., Wenger, P., and Arakelian, V., 2008, "Self Motions of General 3-RPR Planar Parallel Robots," Int. J. Robot. Res., **27**(7), pp. 855–866.

[13] Gosselin, C. M., 1992, "The Optimum Design of Robotic Manipulators Using Dexterity Indices," Robot. Auton. Syst., **9**(4), pp. 213–226.

[14] Rakotomanga, N., Chablat, D., and Caro, S., 2008, "Kinetostatic Performance of a Planar Parallel Mechanism With Variable Actuation," 11th International Symposium on Advances in Robot Kinematics, Kluwer Academic Publishers, Batz-sur-mer, France.
[15] Merlet, J.-P., 2006, "Jacobian, Manipulability, Condition Number, and Accuracy of Parallel Robots," ASME J. Mech. Des., **128** (1), pp. 199–206.
[16] Angeles, J., 2007, Fundamentals of Robotic Mechanical Systems: Theory, Methods, and Algorithms, 3rd ed., Springer, New York.
[17] Alba-Gomez, O., Wenger, P., and Pamanes, A., 2005, "Consistent Kinetostatic Indices for Planar 3-DOF Parallel Manipulators, Application to the Optimal Kinematic Inversion," *Proceedings of ASME 2005 IDETC/CIE Conference*, Long Beach, CA, September 24–28.
[18] Arakelian, V., Briot, S., and Glazunov, V., 2008, "Increase of Singularity-Free Zones in the Workspace of Parallel Manipulators Using Mechanisms of Variable Structure," Mech. Mach. Theory, **43**(9), pp. 1129–1140.
[19] Hubert, J., and Merlet, J.-P., 2008, *Singularity Analysis Through Static Analysis*, *Advances in Robot Kinematics*, Springer, New York, pp. 13–20.
[20] Ranganath, R., Nair, P. S., Mruthyunjaya, T. S., and Ghosal, A., 2004, "A Force–Torque Sensor Based on a Stewart Platform in a Near-Singular Configuration," Mech. Mach. Theory, **39**(9), pp. 971–998.
[21] Alvan, K., and Slousch, A., 2003, "On the Control of the Spatial Parallel Manipulators With Several Degrees of Freedom," Mech. Mach. Theory, **1**, pp. 63–69.
[22] Dasgupta, B., and Mruthyunjaya, T., 1998, "Force Redundancy in Parallel Manipulators: Theoretical and Practical Issues," Mech. Mach. Theory, **33**(6), pp. 724–742.
[23] Glazunov, V., Kraynev, A., Bykov, R., Rashoyan, G., and Novikova, N., 2004, "Parallel Manipulator Control While Intersecting Singular Zones," *Proceedings of the 15th Symposium on Theory and Practice of Robots and Manipulators (RoManSy) CISM-IFToMM*, Montreal.
[24] Kotlarski, J., Do Thanh, T., Abdellatif, H., and Heimann, B., 2008, "Singularity Avoidance of a Kinematically Redundant Parallel Robot by a Constrained Optimization of the Actuation Forces," *Proceedings of the 17th CISM-IFToMM Symposium RoManSy*, pp. 435–442.
[25] Hesselbach, J., Wrege, J., Raatz, A., and Becker, O., 2004, "Aspects on the Design of High Precision Parallel Robots," Assem. Autom., **24**(1), pp. 49–57.
[26] Bhattacharya, S., Hatwal, H., and Ghosh, A., 1998, "Comparison of an Exact and Approximate Method of Singularity Avoidance in Platform Type Parallel Manipulators," Mech. Mach. Theory, **33**(7), pp. 965–974.
[27] Dasgupta, B., and Mruthyunjaya, T., 1998, "Singularity-Free Path Planning for the Steward Platform Manipulator," Mech. Mach. Theory, **33**(6), pp. 715–725.
[28] Kemal Ider, S., 2005, "Inverse Dynamics of Parallel Manipulators in the Presence of Drive Singularities," Mech. Mach. Theory, **40**, pp. 33–44.
[29] Kevin Jui, C. K., and Sun, Q., 2005, "Path Tracking of Parallel Manipulators in the Presence of Force Singularity," ASME J. Dyn. Syst., Meas., Control, **127**, pp. 550–563.
[30] Nenchev, D. N., Bhattacharya, S., and Uchiyama, M., 1997, "Dynamic Analysis of Parallel Manipulators Under the Singularity-Consistent Parameterization," Robotica, **15**(4), pp. 375–384.
[31] Perng, M. H., and Hsiao, L., 1999, "Inverse Kinematic Solutions for a Fully Parallel Robot With Singularity Robustness," Int. J. Robot. Res., **18**(6), pp. 575–583.
[32] Briot, S., and Arakelian, V., 2008, "Optimal Force Generation in Parallel Manipulators for Passing Through the Singular Positions," Int. J. Robot. Res., **27**(8), pp. 967–983.
[33] Briot, S., Arakelian, V., and Guégan, S., 2008, "Design and Prototyping of a Partially Decoupled 4-DOF 3T1R Parallel Manipulator with High-Load Carrying Capacity," ASME J. Mech. Des., **130**(12), p. 122303.
[34] Briot, S., and Arakelian, V., 2010, "On the Dynamic Properties of Flexible Parallel Manipulators in the Presence of Payload and Type 2 Singularities," ASME Conf. Proc., **2**, pp. 1475–1481.
[35] Bouzgarrou, B. C., Ray, P., and Gogu, G., 2005, "New Approach for Dynamic Modelling of Flexible Manipulators," *Proc. IMechE, Part K: J. Multibody Dyn.*, **219**, pp. 285–298.
[36] Khalil, W., and Guegan, S., 2002, "A Novel Solution for the Dynamic Modeling of Gough-Stewart Manipulators," *Proceedings IEEE International Conference on Robotics and Automation*, Washington, DC, May 11–15.
[37] J.-P. Merlet, *Parallel Robots*, Springer, 2nd edition, 2006.
[38] Boyer, F., and Khalil, W., 1996, "Simulation of Flexible Manipulators Using Newton-Euler Inverse Dynamic Model," *Proceedings of the 1996 IEEE International Conference on Robotics and Automation*, Minneapolis, MN.
[39] Spong, M. W., Khorasani, K., and Kokotovic, P. V., 1987, "An Integral Manifold Approach to the Feedback Control of Flexible Joint Robots," IEEE J. Rob. Autom., **3**(4), pp. 291–300.
[40] Liu, X.-J., Wang, J., and Pritschow, G., 2006, "Kinematics, Singularity and Workspace of Planar 5R Symmetrical Parallel Mechanism," Mech. Mach. Theory, **41**(2), pp. 119–144.
[41] Fleming, P. J., and Pashkevich, A., 1985, "Computer Aided Control System Design Using a Multi-Objective Optimisation Approach," *Control 1985 Conference*, Cambridge, UK, pp. 174–179.